

Ceramics fillers enhancing effects on the dielectric properties of poly(vinylidene fluoride) matrix composites prepared by the torque rheometer method



S.A. Riquelme^a, Koduri Ramam^{a,*}, A.F. Jaramillo^b

^a Departamento de Ingeniería de Materiales-DIMAT, Facultad de Ingeniería, Universidad de Concepción, Concepción 4070409, Chile

^b Department of Mechanical Engineering, Universidad de La Frontera, Francisco Salazar 01145, Temuco 4780000, Chile

ARTICLE INFO

Keywords:

Polymer matrix composites (PMCs)
Dielectric properties
PVDF
Barium zirconate titanate – Barium calcium titanate
Potassium Sodium Antimony Niobate – Bismuth Sodium Potassium Zirconate

ABSTRACT

The dielectric properties of ceramic-polymer composites were investigated using different lead-free ferroelectrics, $0.50[\text{Ba}(\text{Zr}_{0.2}\text{Ti}_{0.8})\text{O}_3]-0.50(\text{Ba}_{0.7}\text{Ca}_{0.3})\text{TiO}_3$ (BZT-BCT) and $0.96(\text{K}_{0.48}\text{Na}_{0.52})(\text{Nb}_{0.95}\text{Sb}_{0.05})\text{O}_3-0.04\text{Bi}_{0.5}(\text{Na}_{0.82}\text{K}_{0.18})_{0.5}\text{ZrO}_3$ (KNNS-BNKZ), as fillers to fabricate composites using poly(vinylidene fluoride) (PVDF) as the matrix. The composites were prepared at $x = 35, 45, 50$, and 65 wt\% according to the formulas $x(\text{BZT-BCT})-(1-x)\text{PVDF}$ and $x\text{KNNS-BNKZ}-(1-x)\text{PVDF}$ by applying melt mixing using a torque rheometer and a hot-pressing process. The distribution of the ceramic filler in the PVDF matrix was examined using a scanning electron microscope and X-ray diffraction analysis. Dielectric, ferroelectric, and piezoelectric analyses were also carried out, the results of which are discussed herein. The dielectric constant and dielectric loss were determined for the pure components and for composites with different ceramic contents within the frequency range of 100 Hz–1 MHz. An increase in the BZT-BCT or KNNS-BNKZ amount resulted in an increase in the dielectric constant of the composites, and at RT and a 1 kHz frequency for $x = 65 \text{ wt\%}$, both composites showed the highest dielectric constant (ϵ') of ~ 48 . The piezoelectric coefficient d_{33} reached peaks of 10 pC/N (BZT-BCT/PVDF) and 5 pC/N (KNNS-BNKZ/PVDF) measured 24 h after poling at 100 Hz.

Introduction

In general, polymer materials are unsuitable for use in capacitors owing to their low dielectric constant; however, their mechanical strength, easy processability, and light weight make them good candidates for use in next-generation flexible electronic devices [1–3]. By contrast, ferroelectric ceramics have high dielectric constants but are brittle and require high processing temperatures. Thus, in practice, it is extremely difficult to achieve a combination of good dielectric and mechanical properties with high processability at ambient temperatures in single phase materials [4]. Lead-free ceramic-polymer composites are a viable alternative for improving the dielectric properties of polymeric films owing to their high dielectric constant, flexibility, non-toxicity, and ease of processing through a melt solution, casting, extrusion, injection, and press molding [5–9].

Among the various types of polymers available, polyvinylidene fluoride (PVDF)-based materials are extremely attractive and are commonly used as a composite matrix owing to their high dielectric constant (~ 10 at room temperature), thermal stability, chemical

resistance, good mechanical properties, and extraordinary pyroelectric and piezoelectric properties. In addition, PVDF is a semi-crystalline polymer that exists in four different phases, α , β , γ , and δ , depending on the preparation conditions, making it suitable for various technological applications including capacitors, piezoelectric sensors, and pyroelectric detectors [10–13].

However, recent studies on potassium-sodium niobate (KNN) and barium zirconate titanate (BZT)-based ceramics have determined that the materials can be used as composite ceramic fillers owing to their excellent dielectric and piezoelectric properties, high Curie temperature (T_c), and ferroelectric properties [14–20]. In fact, grain-oriented KNN-based piezoelectric ceramics can exhibit high d_{33} values ranging from 390 to 490 pC/N and T_c ranging from 217 °C to 304 °C [21,22], which can be used to replace lead-based systems. Although Mishra and Kumar studied BZT-BCT/PVDF ceramic-polymer composites [23,24], they applied a different fabrication process and considered the dielectric behavior within a narrow temperature range. In addition, Chi et al. [25] studied BZT-BCT/PVDF but applied nanoparticles and nanofibers as fillers as well as a melt solution fabrication process [26].

* Corresponding authors.

E-mail addresses: silriquelme@udec.cl (S.A. Riquelme), ramamk@udec.cl (K. Ramam).

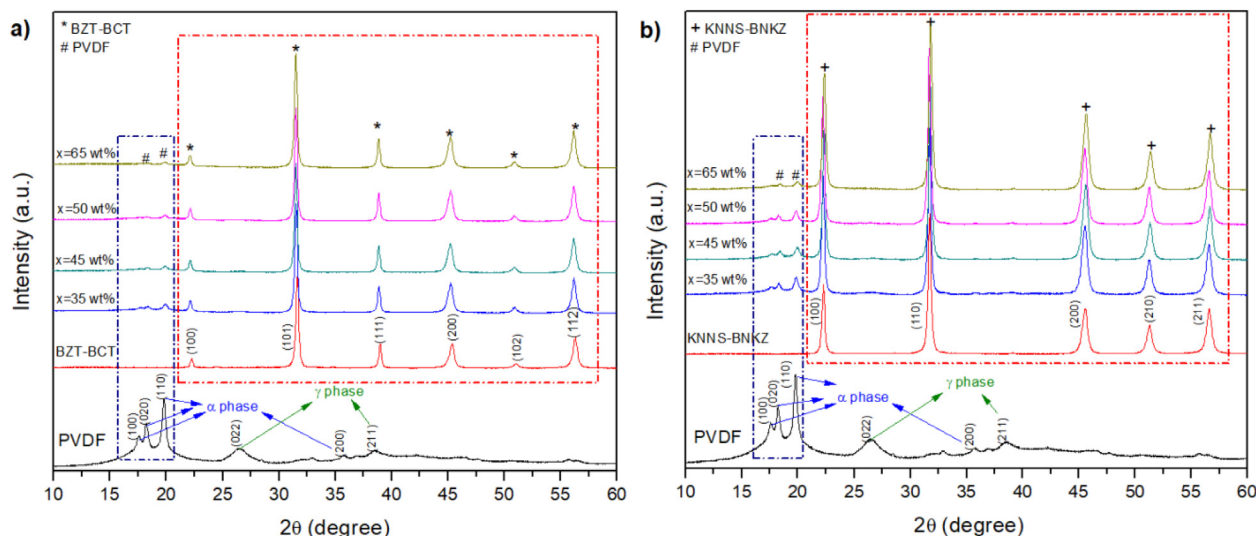


Fig. 1. XRD patterns of (a) PVDF, BZT-BCT and xBZT-BCT-(1-x)PVDF composites and (b) PVDF, KNNS-BNKZ and xKNNS-BNKZ-(1-x)PVDF composites, respectively.

The aim of this study is to compare the dielectric and piezoelectric properties of xBZT-BCT-(1-x)PVDF composites using xKNNS-BNKZ-(1-x)PVDF composites and evaluate their applicability in flexible electronic devices. BZT-BCT and KNNS-BNKZ ceramic powder fillers were incorporated in a PVDF polymer matrix, with different weight fractions forming composites using melt mixing (torque rheometer) and a hot-pressing process. The phase-formation, microstructural, dielectric, ferroelectric, and piezoelectric properties as functions of the ceramic weight fraction, frequency, and temperature were investigated and compared, the results of which are discussed in detail herein.

Experimental

Preparation of ceramic samples

Ceramic samples were synthesized using a solid-state reaction method [19,22]. The starting materials (reactants), i.e., barium carbonate (BaCO_3 , 99% purity), barium zirconate (BaZrO_3 , 99% purity), calcium carbonate (CaCO_3 , 99% purity), and titanium(IV) oxide (TiO_2 , 99% purity) for $0.50[\text{Ba}(\text{Zr}_{0.2}\text{Ti}_{0.8})\text{O}_3]-0.50(\text{Ba}_{0.7}\text{Ca}_{0.3})\text{TiO}_3$ (BZT-BCT), and sodium carbonate (Na_2CO_3 , 99.9% purity), potassium carbonate (K_2CO_3 , 98% purity), niobium(V) oxide (Nb_2O_5 , 99.9% purity), antimony (III) oxide (Sb_2O_5 , 99% purity), bismuth (III) oxide (Bi_2O_3 , 99.9% purity), and zirconium (IV) oxide (ZrO_2 , 99% purity) for $0.96(\text{K}_{0.48}\text{Na}_{0.52})(\text{Nb}_{0.95}\text{Sb}_{0.05})\text{O}_3-0.04\text{Bi}_{0.5}(\text{Na}_{0.82}\text{K}_{0.18})_{0.5}\text{ZrO}_3$ (KNNS-BNKZ), were purchased from Sigma-Aldrich, Germany. The powders were weighed according to a stoichiometric formula, mixed, and ball milled for 24 h using zirconia balls and ethanol in a polyethylene jar. After milling, the mixture was filtered to separate the Zirconia balls, and the resulting powder was dried at 150 °C for 24 h. The dried powders were calcined at 900 °C for 10 h with a heating rate of 5 °C/min, further milled for 12 h, and dried again for 24 h. These calcined powders were pressed into pellets and sintered at 1,350 °C and 1,100 °C for 3 h with a heating rate of 5 °C/min for BZT-BCT and KNNS-BNKZ, respectively. Finally, the sintered pellets were crushed again into a powder using a mortar and pestle for structural experimentation.

Composite preparation

The ceramic-polymer composites were prepared through melt mixing with a torque rheometer (Brabender GmbH & Co., KG model 835205). A PVDF with an average molecular weight of ~534,000, supplied by Sigma-Aldrich, was used as the matrix. For the fabrication of the composites, sintered BZT-BCT and KNNS-BNKZ ceramics were

used as the fillers based on the general formula xBZT-BCT-(1-x)PVDF and xKNNS-BNKZ-(1-x)PVDF (where $x = 35, 45, 50$, and 65 wt%). Mixing was conducted at 200 °C for 10 min under a high shear rate of 60 rpm. Each mixed sample was hot pressed using a Lab-Tech hydraulic press (model LP 20B), at 200 °C for 5 min at 70 bars with preheating and cooling times of 15 and 1 min, respectively, to obtain homogenized composites of 0.4 mm in thickness.

Characterization techniques

X-ray diffraction (XRD) patterns of the ceramic powders, PVDF, and composite samples were analyzed using a Bruker Endeavor X-ray diffractometer (model D4/MAX-Bat, 20 mA and 40 kV) with $\text{Cu-K}\alpha$ radiation of $\lambda = 1.541 \text{ \AA}$ under a low scan rate of 0.02°/min and 2θ ranging from 5° to 90°. A morphological characterization was carried out on all prepared samples using an SEM (Joel Model JSM 6300 LY) with an accelerating voltage of 20 kV. The fractured PVDF and composite specimens were immersed in liquid nitrogen and sputtered-coated with a 50-nm-thick gold layer. For the dielectric measurements, the samples were first gold coated by sputtering to form electrodes on both sides. A precision LCR meter (Agilent E4980A) was used to measure the dielectric properties within a frequency range of 100 Hz–1 MHz and a temperature range of -120 °C–120 °C. After completing the dielectric studies, the ferroelectric properties of the samples were obtained (by applying an external voltage of 10 kV with a frequency of 0.1 Hz) at room temperature using an HP 3325B synthesizer/function generator and a TREK 10/40 high-voltage amplifier. The samples were then poled in a silicon oil bath at 110 °C for 30 min with a dc electric field of 10 kV/mm. The as-poled samples (i.e., samples soon after poling) and samples poled after 24 h were characterized based on their piezoelectric charge coefficient d_{33} at room temperature using a Berlincourt-type meter at 100 Hz.

Results and discussion

X-Ray diffraction (XRD)

Fig. 1(a) and (b) show the XRD patterns of the PVDF and BZT-BCT and KNNS-BNKZ ceramics and composites, respectively. The XRD pattern of the PVDF shows the presence of a semi-crystalline structure, and indicates that the PVDF exists in both mixed α and γ phases together [27,28]. The diffraction peaks at $2\theta = 17.7^\circ, 18.4^\circ, 19.8^\circ$, and 35.8° are assigned to the (1 0 0), (0 2 0), (1 1 0), and (2 0 0) reflections of the α phase PVDF. The diffraction peaks at $2\theta = 26.7^\circ$ and 38.7° are assigned

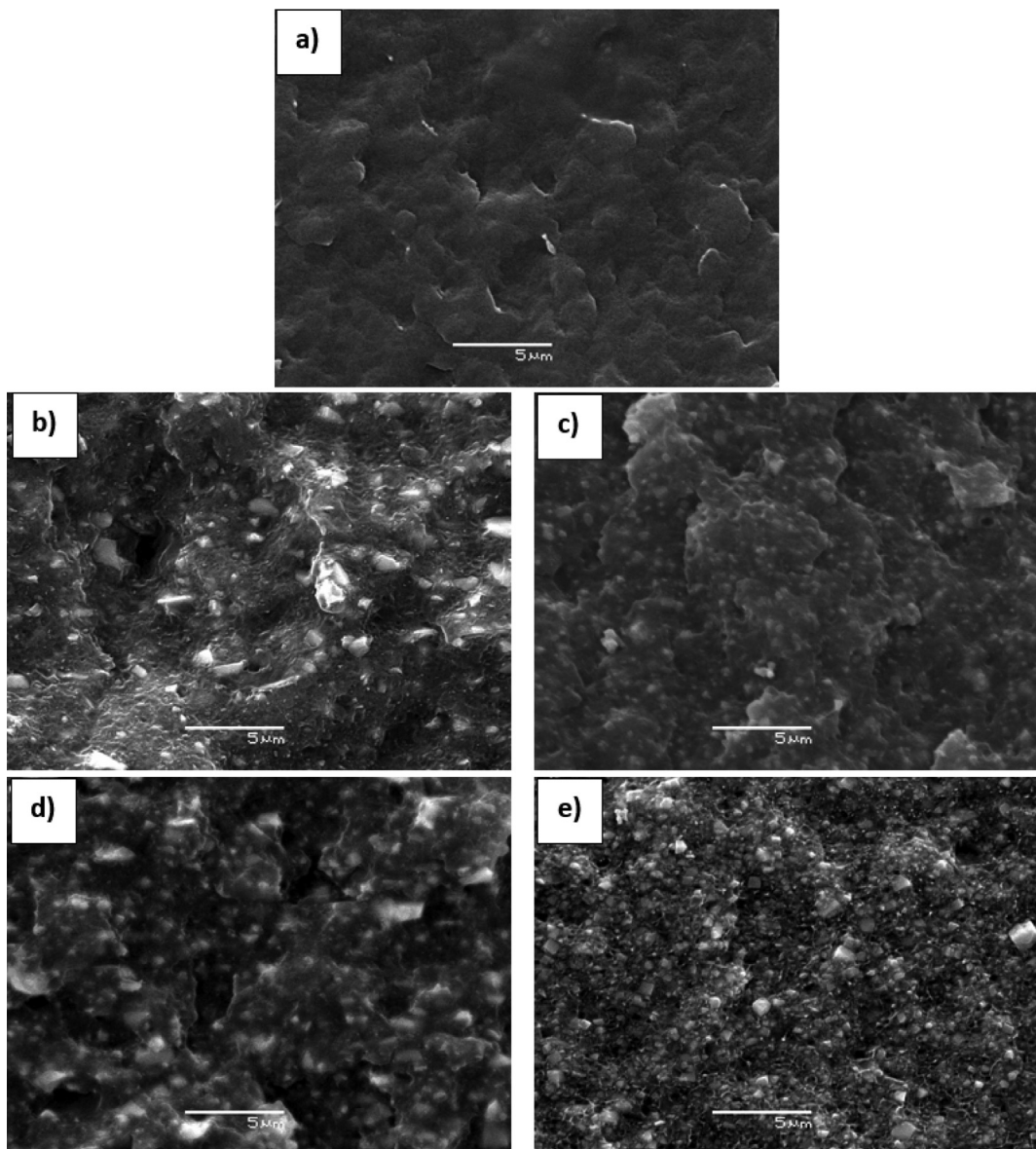


Fig. 2. SEM image of a) fractured cross surface of pure PVDF polymer and composites with a weight fraction of b) 35 wt% BZT-BCT, c) 35 wt% KNNS-BNKZ, d) 65 wt % BZT-BCT, and e) 65 wt% KNNS-BNKZ of ceramic fillers.

to the (0 2 2) and (2 1 1) reflections of the γ phase PVDF [23,28–30]. The diffraction peaks of the sintered BZT-BCT and KNNS-BNKZ ceramic samples show a typical perovskite phase without an unwanted secondary phase, as reported by [21,31–33].

The XRD patterns of all composites demonstrate the presence of ceramics and a PVDF polymer (marked with *, + and #, respectively). When the fraction of ceramic fillers increases in the composites, the peaks of the PVDF gradually reduce and the relative intensity of BZT-BCT and KNNS-BNKZ begin dominating the crystalline nature of the composites. This can be explained as the diffraction intensities of BZT-BCT and KNNS-BNKZ being far higher than those of the PVDF [34].

Scanning electron microscopy (SEM)

Fig. 2 shows the SEM micrographs of the pure PVDF polymer and composites. Fig. 2(a) shows an image of a fractured cross-sectional surface of a PVDF polymer, and it can be seen that the molecules formed a continuous phase without pores inside the matrix, as expected for pure PVDF. Fig. 2(b)–(e) show SEM micrographs of the cross-sections of the composites with different weight fractions of the ceramic

fillers. The ceramic particles BZT-BCT and KNNS-BNKZ are uniformly distributed and surrounded by the PVDF matrix, which is an indication of a typical 0–3 connectivity pattern [23], and the uniform distribution increases with an increase in the ceramic fillers in the PVDF matrix. Ceramic-polymer composites can be classified into different types depending on the connectivity pattern between the ceramic and polymer phases. In the case of 0–3 ceramic-polymer composites, the ceramic particles are connected in zero dimensions in a three-dimensionally interconnected polymer matrix, which means that the composite consists of separated ceramic particles randomly dispersed in a polymer matrix [9]. Thus, the connectivity pattern the dispersion of fillers plays a significant role in the dielectric properties of the composites, and a good dispersion is likely to contribute to excellent dielectric properties, as previously reported [27,29]. The images also indicate that the ceramic fillers have different particle sizes at the micrometer scale, which can be attributed to the hand grinding process.

As reported by Dang et al. [5], a torque rheometer method was selected owing to its good dispersive and distributive mixing capabilities. A torque rheometer method is generally the most popular fabrication route when using a thermoplastic polymer as a matrix

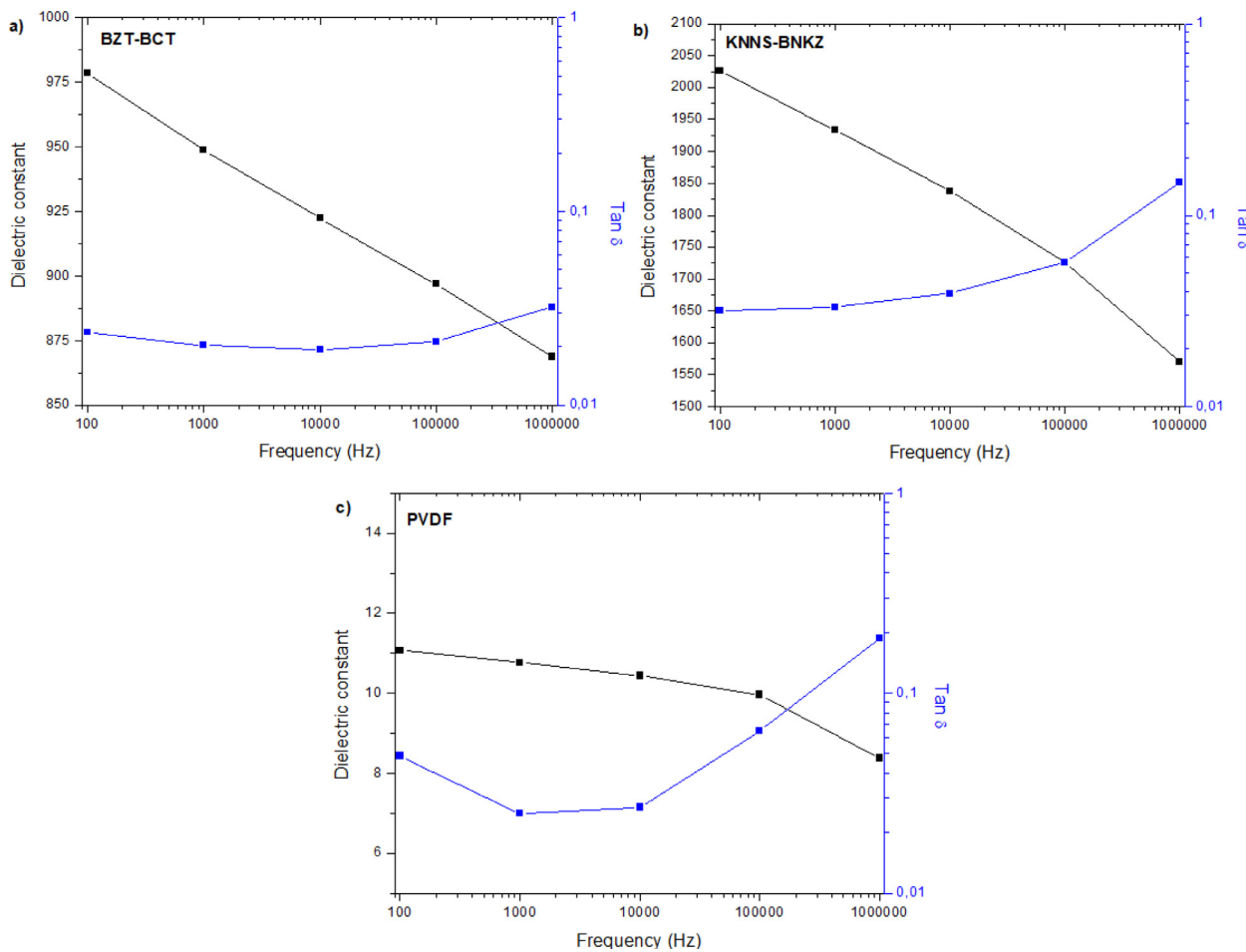


Fig. 3. Variation in dielectric constant and dielectric loss ($\tan \delta$) with frequency for (a) BZT-BCT, (b) KNNS-BNKZ ceramics, and (c) pure PVDF polymer at RT.

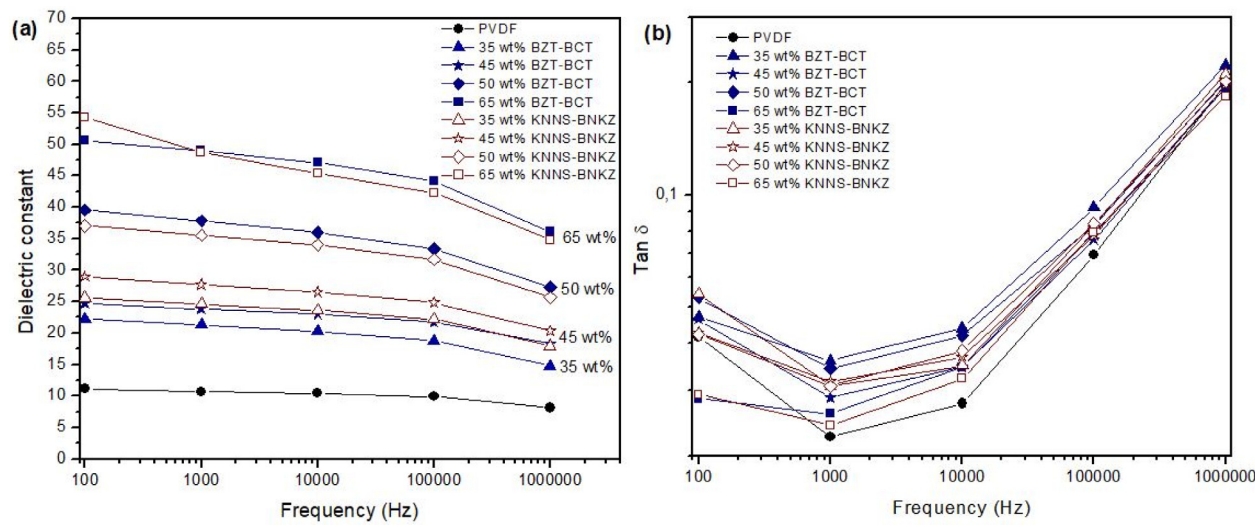


Fig. 4. Variation of (a) dielectric constant and (b) dielectric loss ($\tan \delta$) with frequency for x BZT-BCT-(1- x)PVDF and x KNNS-BNKZ-(1- x)PVDF composites at RT.

owing to its simple technique (it is not necessary to use a solvent) and wide application in practical production because of its convenience, low cost, and mass production capability [35]. In fact, Rawat et al. [28], Behera et al. [34], and Thongbai et al. [36], using hot pressing and solution casting methods instead, obtained composites with pores and an agglomeration, leading to a poor dispersion and weak interfacial interaction between the fillers and polymer matrices.

Frequency dependence of dielectric properties

Fig. 3 shows the frequency dependence of both the dielectric constant and dielectric loss ($\tan \delta$) for ceramic samples and a pure PVDF polymer. The RT values of the dielectric constant and dielectric loss of the ceramic samples at a frequency of 1 kHz were found to be ~ 945 and 0.020 for BZT-BCT and ~ 1933 and 0.033 for KNNS-BNKZ, and for a pure PVDF polymer were determined to be ~ 10.77 and 0.025. The

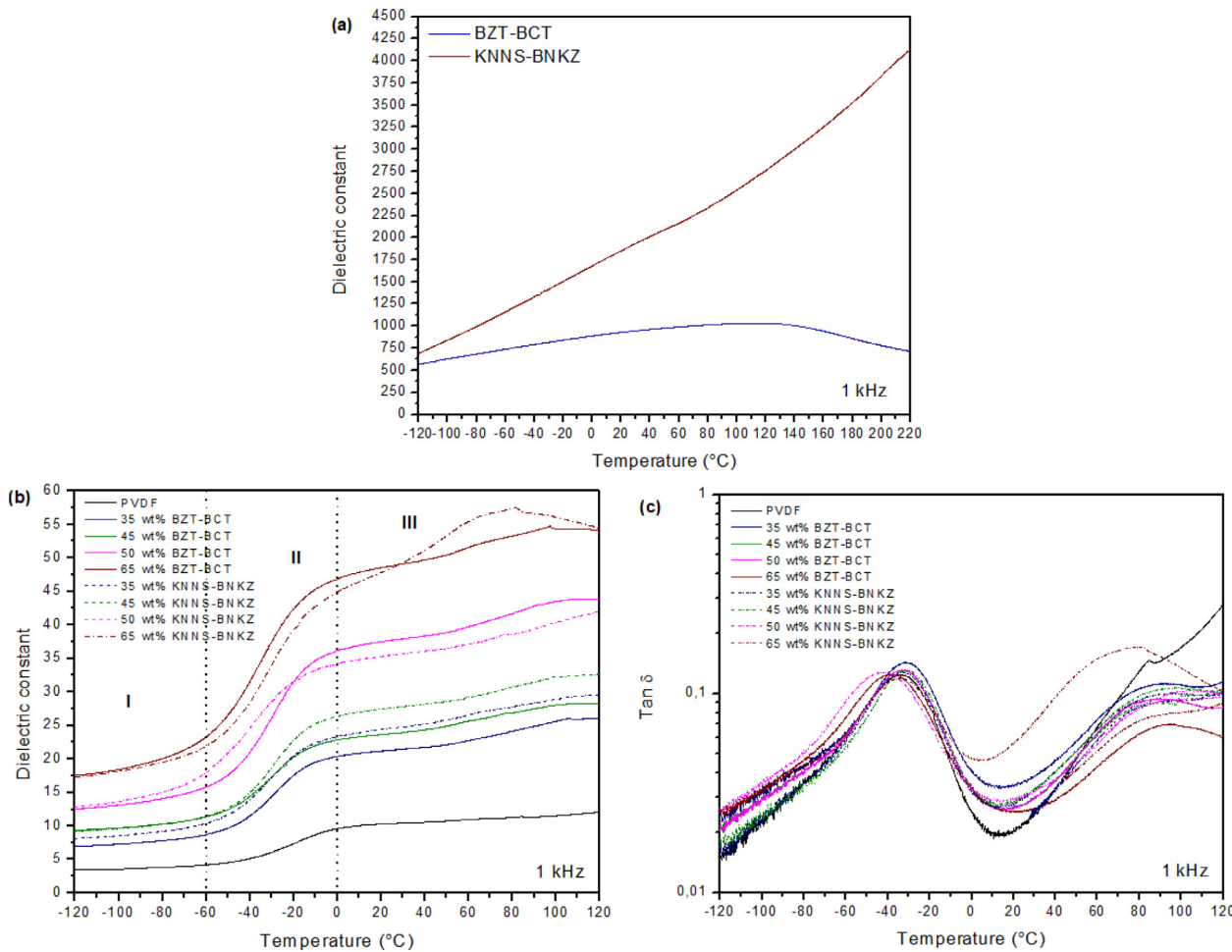


Fig. 5. Variation in dielectric constant with a temperature of (a) BZT-BCT and KNNS-BNKZ and (b) dielectric constant and (c) dielectric loss ($\tan \delta$) of pure PVDF, xBZT-BCT-(1-x)PVDF, and xKNNS-BNKZ-(1-x)PVDF composites at a frequency of 1 kHz.

dielectric constant for the PVDF is mostly frequency independent and for ceramics decreases with frequency. In the case of ceramics, a decrease in the dielectric constant may occur owing to a decrease in polarization with an increase in frequency, as reported by Mishra et al. [23].

By contrast, the dielectric loss for the BZT-BCT decreases from 100 Hz to 10 kHz and then starts increasing at 1 MHz, whereas for KNNS-BNKZ ceramics it continuously increases with the frequency. For the PVDF, the dielectric loss decreases within a low-frequency range of 100 Hz to 1 kHz and then starts increasing from 1 MHz. This behavior is explained by the dielectric relaxation, which is a typical characteristic of such PVDF-based nonlinear dielectrics, as reported by Zhu and Wang [37,38].

The dielectric performances of BZT-BCT/PVDF and KNNS-BNKZ/PVDF composites with different weight fractions were measured. The frequency ranged from 100 Hz to 1 MHz at room temperature. Fig. 4(a) shows the dielectric constants of pure PVDF, BZT-BCT/PVDF, and KNNS-BNKZ/PVDF composites. As expected, the dielectric constant of all composites increases in comparison with pure PVDF but is much lower than for pure ceramics, as previously reported [28]. This remarkable enhancement in dielectric constant can be attributed to the higher dielectric constant of the ceramics and the Maxwell-Wagner-Sillars (MWS) interfacial polarization, which is mainly caused by the large difference in the dielectric constant and conductivity between the fillers and polymer matrix. By contrast, the values of the dielectric constant continuously decrease with an increase in frequency for all composites [8,38–40].

Fig. 4(b) shows the dielectric loss ($\tan \delta$) of pure PVDF, BZT-BCT/PVDF, and KNNS-BNKZ/PVDF composites. It can be seen that the dielectric loss behavior of the composites is again dominated by the PVDF, decreasing within the 100 Hz to 1 kHz frequency range, and then continuously increases at up to a 1 MHz frequency. The decrease in dielectric loss at a lower frequency with the relaxation peak centered at around 10 Hz (α_c relaxation) is attributed to the dipole relaxation along the chain axes of the α -form. By contrast, the increase in the dielectric loss at high frequency with a relaxation peak at approximately 1 MHz (α_a relaxation) is attributed to both amorphous dipoles and dipoles at the crystal/amorphous interfaces, as reported by Zhu and Wang [29,38,41].

In recent studies, composites were fabricated in an attempt to incorporate oriented fillers into the matrix. You et al. [42] demonstrated a large enhancement of the dielectric constant of CCTO/epoxy composites based on a CCTO skeleton sintered at different temperatures. The authors found a high dielectric constant of 1091, 1600, and 1936, and the dielectric loss was found to be between approximately 0.5 and 1.5 for 49.8, 54.1, and 57.7 vol% of the CCTO at 1 kHz. As shown, this method is a good alternative for obtaining a high dielectric constant in ceramic-polymer composites.

It is clear that the much higher KNNS-BNKZ dielectric constant in comparison to that of the BZT-BCT is not reflected in the dielectric constant of the composite. In fact, for high ceramic weight concentrations it was found that xBZT-BCT-(1-x)PVDF achieves a higher dielectric constant.

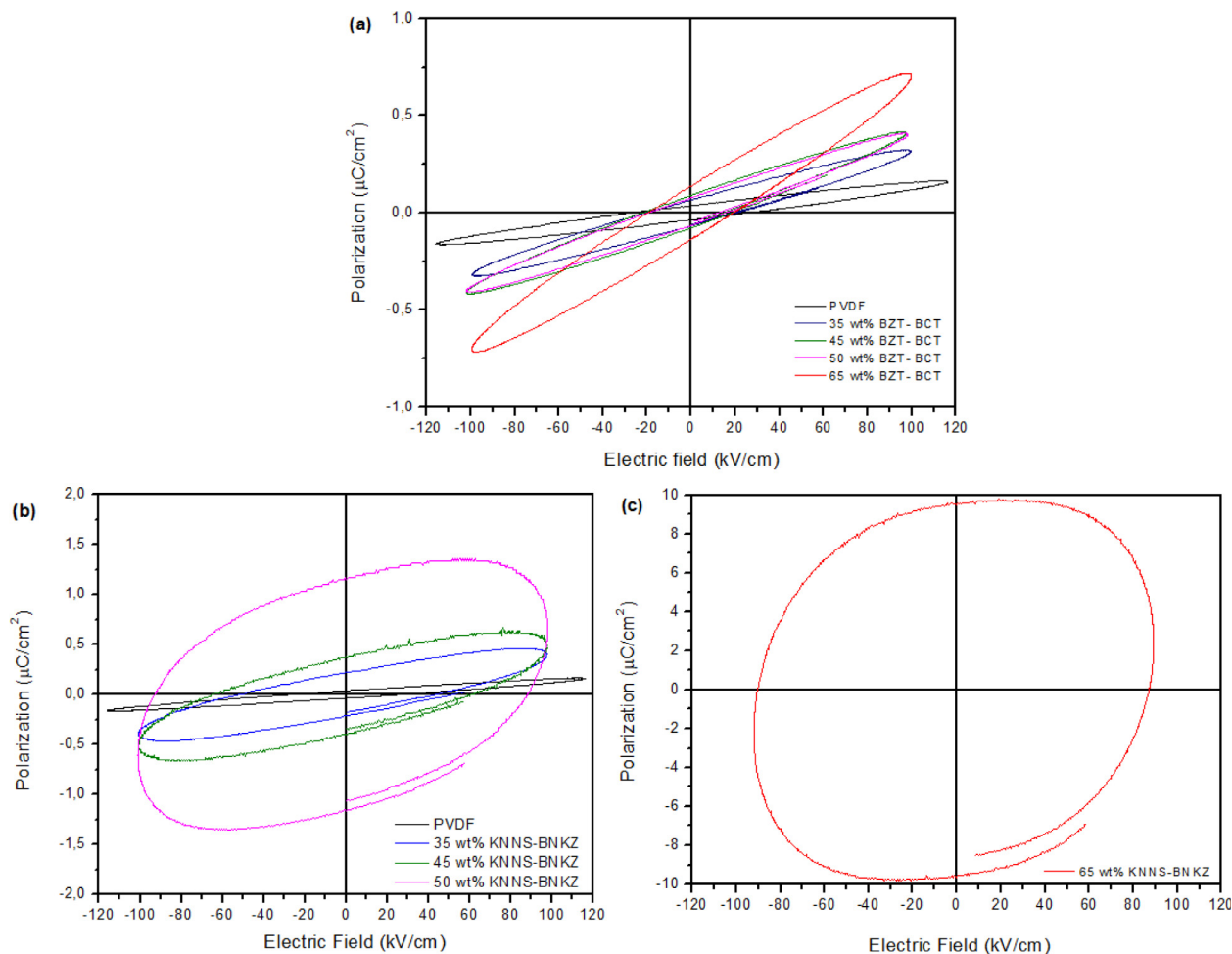


Fig. 6. P-E hysteresis loop of (a) xBZT-BCT-(1-x)PVDF and (b)(c) xKNNS-BNKZ-(1-x)PVDF composites.

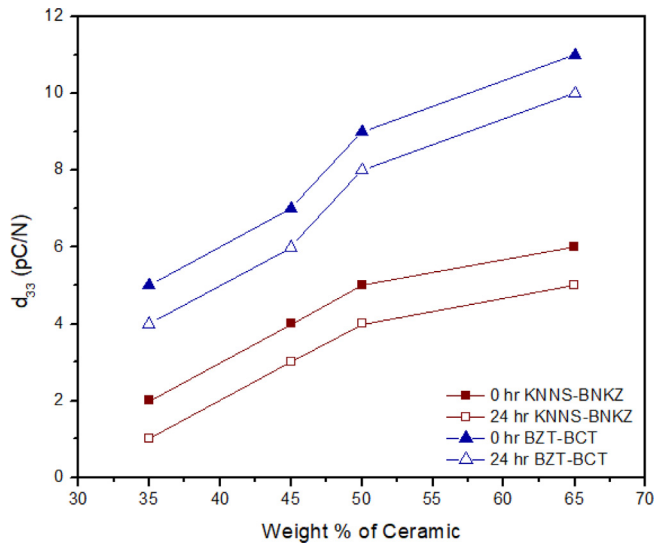


Fig. 7. Piezoelectric coefficient (d_{33}) of xBZT-BCT-(1-x)PVDF and xKNNS-BNKZ-(1-x)PVDF composites at RT.

Temperature dependence of dielectric properties

Fig. 5(a) shows the dielectric constant as a function of temperature at a 1 kHz frequency for the ceramic samples. As shown, the dielectric constant increases with temperature. The RT value for a dielectric

constant at 1 kHz is approximately 945 for BZT-BCT and 1933 for KNNS-BNKZ, and at 120 °C the value increases to approximately 1041 for BZT-BCT and 2735 for KNNS-BNKZ. In the case of BZT-BCT, the dielectric constant reaches the maximum, and then decreases from the 120 °C temperature of the T_c [19].

Fig. 5(b) and (c) show the temperature dependence of the dielectric constant and dielectric loss ($\tan \delta$) at a frequency of 1 kHz for the pure PVDF and the BZT-BCT/PVDF and KNNS-BNKZ/PVDF composites, respectively. As the figure indicates, three stages can be identified. The first is from -120 °C to -60 °C, where the dielectric constant for the PVDF and the composites is mostly independent of the temperature, indicating that the relaxation processes governing the dielectric constant are also unaffected by the temperature [34]. The second stage is identified within the range of -60 °C to 0 °C, where it is possible to see a step in the behavior owing to the glass transition of the PVDF at approximately -38 °C, and owing to the relaxation processes in the PVDF [34,38,43]. Finally, during the third stage, from 0 °C to 120 °C, the value of the dielectric constant increases continuously for the dipole and interfacial polarization induced by the ceramic filler and the thermal expansion of the PVDF matrix and ceramic [10].

In the dielectric loss, two peak regions can be seen, namely, from -60 °C to 0 °C and from 70 °C to 110 °C. The peak at low temperature can be explained from the rich relaxation processes of the PVDF. By contrast, the high-temperature peak is mainly caused by the interfacial relaxation arising from the ceramic–polymer interfaces [41].

Ferroelectric studies

Fig. 6 shows the ferroelectric polarization versus the external electric field (P-E) hysteresis behavior of pure PVDF and the xBZT-BCT-(1-x)PVDF and xKNNS-BNKZ-(1-x)PVDF composites. The results indicate that the PVDF and composites exhibit a lossy capacitor behavior without a saturation polarization (P_s). The PVDF shows a weak P-E loop, which is consistent with the presence of α and γ phases in the material, as confirmed through the XRD analysis. In the case of the composites, by increasing the BZT-BCT and KNNS-BNKZ ceramic fillers, the heterogeneous polarization facilitates the charge accumulation at the interface of the composites [44]. For the PVDF polymer and composites, it can be observed that the remanence polarization (Pr) increases with an increase in the amount of ceramic fillers from $0.038 \mu\text{C}/\text{cm}^2$ for pure PVDF, with a ceramic filler of 65 wt% for both composites, to $0.139 \mu\text{C}/\text{cm}^2$ for BZT-BCT and to $9.508 \mu\text{C}/\text{cm}^2$ for KNNS-BNKZ.

In summary, these results indicate that the polarization response of the xBZT-BCT-(1-x)PVDF and xKNNS-BNKZ-(1-x)PVDF composites is significantly influenced by the incorporation of the ceramic filler particles within the PVDF matrix.

Piezoelectric studies

Fig. 7 shows the piezoelectric charge coefficient (d_{33}) for the xBZT-BCT-(1-x)PVDF and xKNNS-BNKZ-(1-x)PVDF composites with ceramic filler weight fractions of 35, 45, 50, and 65 wt% immediately and after 24 h of poling and at RT. It can be observed in the figure that the value of d_{33} increases with the amount of the ceramic filler, as reported by Zhang et al. [45], and Jain et al. [46]. As expected, the values measured 24 h after poling were slightly lower than the values recorded immediately after poling, which is due to the samples reaching the remnant polarization gradually over time, forcing some of the dipoles to return to their original position.

As reported by Thongsanitgarn et al. [47], the value of the piezoelectric coefficient (d_{33}) for the PZT/PVDF composites was 16 pC/N (90/10 wt%). This was probably due to the different electric field used to pole the sample prior to the d_{33} measurement. A similar result was found by Renxin et al. [48] who reported a d_{33} value of approximately 15.5 pC/N for the PZT/PVDF composite (80/20 vol%). Finally, Pandey et al. [49] reported a d_{33} value of approximately 27.3 pC/N for the BCT-BZT/PVDF composite (25/75 wt%). In our case, the d_{33} value immediately after the poling was 11 pC/N for BZT-BCT and 6 pC/N for KNNS-BNKZ, whereas 24 h after poling it was reduced to 10 pC/N for BZT-BCT and 5 pC/N for KNNS-BNKZ with a ceramic filler of 65 wt% for both composites.

Conclusions

Piezoelectric BZT-BCT/PVDF and KNNS-BNKZ/PVDF 0–3 composites having a ceramic filler with weight fractions of 35%, 45%, 50%, and 65% were prepared through melt mixing and a hot press method, and characterized regarding their dielectric, ferroelectric, and piezoelectric properties. The XRD patterns showed sharp peaks corresponding to both the polymer and ceramic material. The SEM results showed that the melt mixing torque rheometer method allows composites with a homogeneous dispersion of fillers to be obtained.

The dielectric constant of all composites decreased with an increase in frequency, which can be attributed to the polarization relaxation, the interface polarization, and the dipole orientation polarization in the inner structure of the composites. The increase in the dielectric constant with an increase in the temperature and amount of ceramic filler was attributed to the dipole and interfacial polarization induced by the filler, as well as to the thermal expansion of the PVDF matrix and ceramic. Regarding the polarization response, the results indicate that it is significantly influenced by the incorporation of ceramic filler particles within the PVDF matrix. However, the piezoelectric coefficient

increased with the amount of ceramic filler. Finally, it was concluded that the PVDF dominates the dielectric and piezoelectric behavior of the composites, and to obtain better properties, the PVDF processing method needs to be improved to allow the occurrence of a β -phase.

Declaration of Competing Interest

The authors declare that they have no known competing financial interests or personal relationships that could have appeared to influence the work reported in this paper.

Acknowledgments

Financial supported by the National Commission for Scientific and Technological Research (CONICYT) for the CONICYT-PFCHA/National Doctorate 2014-21140951 scholarship for Materials Science and Engineering at UdeC, project FONDEF ID15I10312 of National Commission for Scientific and Technological Research (CONICYT) and Project CORFO 15IPPID 45708 of Production Development Corporation (CORFO). The authors also would like to thank the Electroactive oxides for smart devices group of the Materials Department for information technologies of Instituto de Ciencia de Materiales de Madrid (ICMM), of Consejo Superior de Investigaciones Científicas (CSIC, Spain).

References

- [1] Mao X, Guo W, Li C, Yang J, Du L, Hu W, et al. Low-temperature synthesis of polyimide/poly(vinylidene fluoride) composites with excellent dielectric property. *Mater Lett* 2017;193:213–5. <https://doi.org/10.1016/j.matlet.2017.01.065>.
- [2] Ramadan KS, Sameoto D, Evoy S. A review of piezoelectric polymers as functional materials for electromechanical transducers. *Smart Mater Struct* 2014;23. <https://doi.org/10.1088/0964-1726/23/3/033001>.
- [3] Samanta B, Kumar P, Nanda D, Sahu R. Dielectric properties of Epoxy-Al composites for embedded capacitor applications. 102384 *Results Phys* 2019;14. <https://doi.org/10.1016/j.rinp.2019.102384>.
- [4] Gajula GR, Chidambara Kumar KN, Buddiga LR, Nethala GP. Dielectric and impedance properties of $\text{Li}_{0.5}\text{Fe}_{2.5}\text{O}_4$ doped BaTiO_3 composite ceramics. *Results Phys* 2018;11:899–904. <https://doi.org/10.1016/j.rinp.2018.10.057>.
- [5] Dang ZM, Yuan JK, Zha JW, Zhou T, Li ST, Hu GH. Fundamentals, processes and applications of high-permittivity polymer-matrix composites. *Prog Mater Sci* 2012;57:660–723. <https://doi.org/10.1016/j.pmatsci.2011.08.001>.
- [6] Fu J, Hou Y, Zheng M, Wei Q, Zhu M, Yan H. Improving dielectric properties of PVDF composites by employing surface modified strong polarized BaTiO_3 particles derived by molten salt method. *ACS Appl Mater Interfaces* 2015;7:24480–91. <https://doi.org/10.1021/acsami.5b05344>.
- [7] Bai Y, Cheng ZY, Bharti V, Xu HS, Zhang QM. High-dielectric-constant ceramic-powder polymer composites. *Appl Phys Lett* 2000;76:3804–6. <https://doi.org/10.1063/1.126787>.
- [8] Wang Z, Fang M, Li H, Wen Y, Wang C, Pu Y. Enhanced dielectric properties in poly(vinylidene fluoride) composites by nanosized $\text{Ba}(\text{Fe 0.5 Nb 0.5})\text{O}_3$ powders. *Compos Sci Technol* 2015;117:410–6. <https://doi.org/10.1016/j.compscitech.2015.07.018>.
- [9] Mishra P, Kumar P. Dielectric properties of $\Phi(\text{BZT-BCT})-(1-\Phi)$ epoxy composites with 0–3 connectivity. *Adv Condens Matter Phys* 2013;2013.. <https://doi.org/10.1155/2013/858406>.
- [10] Li M, Wondergem HJ, Spijkman MJ, Asadi K, Katsouras I, Blom PWM, et al. Revisiting the δ -phase of poly(vinylidene fluoride) for solution-processed ferroelectric thin films. *Nat Mater* 2013;12:433–8. <https://doi.org/10.1038/nmat3577>.
- [11] Sharma M, Gaur A, Kumar J. Temperature-dependent dielectric response of (1-x) PVDF / (x) BaTiO_3 3 nanocomposite films. *Phys B Condens Matter* 2019;563:23–9.
- [12] Zhang Q, Gao F, Hu G, Zhang C, Wang M, Qin M, et al. Characterization and dielectric properties of modified $\text{Ba}0.6\text{Sr}0.4\text{TiO}_3/\text{PVF}$ (Vinylidene Fl Uoride) composites with high dielectric tunability. *Compos Sci Technol* 2015;118:94–100. <https://doi.org/10.1016/j.compscitech.2015.08.013>.
- [13] Santos IA, Rosso JM, Ctrica LF, Bonadio TGM, Freitas VF, Guo R, et al. Dielectric and structural features of the environmentally friendly lead-free PVDF/Ba0.3Na0.7Ti0.3Nb0.7O3 0–3 composite. *Curr Appl Phys* 2016;16:1468–72. <https://doi.org/10.1016/j.cap.2016.08.016>.
- [14] Hanani Z, Mezzane D, Amjoud M, Fourcade S, Razumnyaya AG, Luk'yanchuk IA, et al. Enhancement of dielectric properties of lead-free BCZT ferroelectric ceramics by grain size engineering. *Superlattices Microstruct* 2019;127:109–17. <https://doi.org/10.1016/j.spmi.2018.03.004>.
- [15] Bao H, Zhou C, Xue D, Gao J, Ren X. A modified lead-free piezoelectric BZT-xBCt system with higher Tc. *J Phys D Appl Phys* 2010. <https://doi.org/10.1088/0022-3727/43/46/465401>.
- [16] Liu W, Ren X. Large piezoelectric effect in Pb-free ceramics. *Phys Rev Lett* 2009;103:103.257602. <https://doi.org/10.1103/PhysRevLett>.
- [17] Zhang Y, Wang S, Chen C, Zhang N, Wang A, Zhu Y, et al. Enhanced linearity of

KNNS-BNKZ ceramics by combining the controls of phase composition and microstructure. *Ceram Int* 2018;44:8380–6. <https://doi.org/10.1016/j.ceramint.2018.02.030>.

[18] Zhang Y, Wang S, Chen C, Zhang N, Wang A, Zhu Y, et al. Reduced hysteresis of KNNS-BNKZ piezoelectric ceramics through the control of sintering temperature. *Ceram Int* 2018;44:12435–41. <https://doi.org/10.1016/j.ceramint.2018.04.033>.

[19] Mishra P, Sonia S, Kumar P. Effect of sintering temperature on dielectric, piezoelectric and ferroelectric properties of BZT-BCT 50/50 ceramics. *J Alloys Compd* 2012;545:210–5. <https://doi.org/10.1016/j.jallcom.2012.08.017>.

[20] Riquelme S, Ramam K. Dielectric and piezoelectric properties of lead free BZT-BCT/PVDF flexible composites for electronic applications. *Mater Res Express* 2019. <https://doi.org/10.1088/2053-1591/ab522c>.

[21] Li YM, Shen ZY, Liu YJ, Shen WC, Wang ZM. High piezoelectric response in KNNS-xBNKZ lead-free ceramics. *J Mater Sci Mater Electron* 2015;26:9817–20. <https://doi.org/10.1007/s10854-015-3654-3>.

[22] Ou-Yang J, Zhu B, Zhang Y, Chen S, Yang X, Wei W. New KNN-based lead-free piezoelectric ceramic for high-frequency ultrasound transducer applications. *Appl Phys A Mater Sci Process* 2015;118:1177–81. <https://doi.org/10.1007/s00339-015-9004-8>.

[23] Kumar P, Mishra P, Sonia S. Synthesis and Characterization of Lead-Free Ferroelectric 0.5[Ba(Zr0.2Ti0.8)O3]–0.5[Ba(0.7Ca0.3)TiO3]–Polyvinylidene Difluoride 0–3 Composites. *J Inorg Organomet Polym Mater* 2013;23:539–45. <https://doi.org/10.1007/s10904-012-9809-2>.

[24] Mishra P, Kumar P. Dielectric properties of 0.25(BZT-BCT)-0.75[(1-x)PVDF-xCCTO] (x=0.02, 0.04, 0.06, 0.08 and 0.1) composites for embedded capacitor applications. *Compos Sci Technol* 2013;88:26–32. <https://doi.org/10.1016/j.compscitech.2013.08.020>.

[25] Chi Q, Liu G, Zhang C, Cui Y, Wang X, Lei Q. Microstructure and dielectric properties of BZT-BCT/PVDF nanocomposites. *Results Phys* 2018;8:391–6. <https://doi.org/10.1016/j.rinp.2017.12.052>.

[26] Chi QG, Dong JF, Liu GY, Chen Y, Wang X, Lei QQ. Effect of particle size on the dielectric properties of 0.5Ba(Zr 0.2 Ti 0.8)O 3–0.5Ba (0.7 Ca 0.8)TiO 3 /polyvinylidene fluoride hybrid films. *Ceram Int* 2015;41:15116–21. <https://doi.org/10.1016/j.ceramint.2015.08.083>.

[27] Patel PK, Yadav KL, Dutta S. Development of Ba0.95Sr0.05(Fe0.5Nb0.5)O3/poly(vinylidene fluoride) nanocomposites for energy storage. *J Mater Sci Mater Electron* 2015;26:4165–71. <https://doi.org/10.1007/s10854-015-2961-z>.

[28] Rawat M, Yadav KL. Dielectric, enhanced magnetic and magnetodielectric properties of hot pressed (BNBT-BFO)/PVDF composite films. *J Polym Res* 2015;22:1–7. <https://doi.org/10.1007/s10965-015-0874-4>.

[29] Thomas P, Varughese KT, Dwarakanath K, Varma KBR. Dielectric properties of Poly(vinylidene fluoride)/CaCu3Ti4O12 composites. *Compos Sci Technol* 2010;70:539–45. <https://doi.org/10.1016/J.COMPSCITECH.2009.12.014>.

[30] Martins P, Lopes AC, Lanceros-Mendez S. Electroactive phases of poly(vinylidene fluoride): determination, processing and applications. *Prog Polym Sci* 2014;39:683–706. <https://doi.org/10.1016/j.progpolymsci.2013.07.006>.

[31] Sreenivas Puli V, Pradhan DK, Pérez W, Katiyar RS. Structure, dielectric tunability, thermal stability and diffuse phase transition behavior of lead free BZT-BCT ceramic capacitors. *J Phys Chem Solids* 2013;74:466–75. <https://doi.org/10.1016/j.jpcs.2012.11.012>.

[32] Yu L, Xi H, Yu Z, Liu Y, Lyu Y. Giant strain response with low hysteresis in potassium sodium niobate based lead-free ceramics. *Ceram Int* 2019;45:14675–83. <https://doi.org/10.1016/j.ceramint.2019.04.187>.

[33] Jayakrishnan AR, Alex KV, Thomas A, Silva JPB, Kamakshi K. Composition-dependent xBa(Zr0.2Ti0.8)O3-(1-x)(Ba0.7Ca0.3)TiO3 bulk ceramics for high energy storage applications. *Ceram Int* 2019;45:5808–18.

[34] Behera C, Choudhary RNP, Das PR. Development of multiferroic polymer nanocomposite from PVDF and (Bi0.5Ba0.25Sr0.25)(Fe0.5Ti0.5)O3. *J Mater Sci Mater Electron* 2016;28:2586–97. <https://doi.org/10.1007/s10854-016-5834-1>.

[35] Dias CJ, Das-Gupta DK. Inorganic ceramic / polymer ferroelectric composite electrets. *IEEE Trans Dielectr Electr Insul* 1996;3:706–34.

[36] Silakae K, Sajijingwong W, Meeporn K, Maensiri S, Thongbai P. Effects of processing methods on dielectric properties of BaTiO3/poly(vinylidene fluoride) nanocomposites. *Microelectron Eng* 2015;146:1–5. <https://doi.org/10.1016/j.mee.2015.01.029>.

[37] Fukada E, Furukawa T. Piezoelectricity and ferroelectricity in polyvinylidene fluoride. *Ultrasonics* 1981;19:31–9. [https://doi.org/10.1016/0041-624X\(81\)90030-5](https://doi.org/10.1016/0041-624X(81)90030-5).

[38] Zhu L, Wang Q. Novel ferroelectric polymers for high energy density and low loss dielectrics. *Macromolecules* 2012;45:2937–54. <https://doi.org/10.1021/ma2024057>.

[39] Wang Q, Zhu L. Polymer nanocomposites for electrical energy storage. *J Polym Sci Part B Polym Phys* 2011;49:1421–9. <https://doi.org/10.1002/polb.22337>.

[40] Mendes SF, Costa CM, Serra RS, Baldalo AA, Sencadas V, Gomez-Ribelles JL, et al. Influence of filler size and concentration on the low and high temperature dielectric response of poly(Vinylidene fluoride)/Pb(Zr 0.53 Ti 0.47)O 3 composites. *J Polym Res* 2012;19. <https://doi.org/10.1007/s10965-012-9967-5>.

[41] Chanmal CV, Jog JP. Dielectric relaxations in PVDF/BaTiO3 nanocomposites. *Express Polym Lett* 2008;2:294–301. <https://doi.org/10.3144/expresspolymlett.2008.35>.

[42] You X, Chen N, Du G. Constructing three-dimensionally interwoven structures for ceramic/polymer composites to exhibit colossal dielectric constant and high mechanical strength: CaCu 3 Ti 4 O 12 /epoxy as an example. *Compos Part A Appl Sci Manuf* 2018;105:214–22. <https://doi.org/10.1016/j.compositesa.2017.11.025>.

[43] Wang S, Sun J, Tong L, Guo Y, Wang H, Wang C. Superior dielectric properties in Na0.35%Ba99.65%Ti99.65%Nb0.35%O3/PVDF composites. *Mater Lett* 2018;211:114–7. <https://doi.org/10.1016/j.matlett.2017.09.099>.

[44] Sharma M, Quamarra JK, Gaur A. Behaviour of multiphase PVDF in (1-x)PVDF/(x)BaTiO3 nanocomposite films: structural, optical, dielectric and ferroelectric properties. *J Mater Sci Mater Electron* 2018;29:10875–84. <https://doi.org/10.1007/s10854-018-9163-4>.

[45] Zhang DQ, Wang DW, Yuan J, Zhao QL, Wang ZY, Cao MS. Structural and electrical properties of PZT/PVDF piezoelectric nanocomposites prepared by cold-press and hot-press routes. *Chinese Phys Lett* 2008;25:4410–3. <https://doi.org/10.1088/0256-307X/25/12/063>.

[46] Jain A, Prashanth KJ, Sharma AK, Jain A, Rashmi Pn. Dielectric and piezoelectric properties of PVDF/PZT composites: a review. *Polym Eng Sci* 2015;55:1589–616. <https://doi.org/10.1002/pen.24088>.

[47] Thongsanitgarn P, Watcharapasorn A, Jiansirisomboon S. Electrical and mechanical properties of PZT/PVDF 0–3 composites. *Surf Rev Lett* 2010;17:1–7. <https://doi.org/10.1142/S0218625X10013540>.

[48] Renxin W, Wen C, Jing Z, Yueming L, Huajun S. Dielectric and piezoelectric properties of 0–3 PZT/PVDF composite doped with polyaniline. *J Wuhan Univ Technol Mater Sci Ed* 2006;21:84–7. <https://doi.org/10.1007/bf02861478>.

[49] Pandey BK, Kumar A, Chandra KP, Kulkarni AR, Jayaswal SK, Prasad K. Electrical properties of 0–3 0.5(Ba0.7Ca0.3)TiO 3–0.5Ba(Zr0.2Ti0.8)O 3 /PVDF nanocomposites. *J Adv Dielectr* 2018;08:1850027. <https://doi.org/10.1142/s2010135x18500273>.